



Article

Relativistic Effects on NMR Parameters of Halogen-Bonded Complexes

Ibon Alkorta ^{1,*}, José Elguero ¹, Manuel Yáñez ², Otilia Mó ² and M. Merced Montero-Campillo ^{2,*}

¹ Instituto de Química Médica, IQM-CSIC. Juan de la Cierva, 3, 28006 Madrid, Spain; iqmbe17@iqm.csic.es

² Departamento de Química, Módulo 13, Facultad de Ciencias and Institute of Advanced Chemical Sciences (IadChem), Universidad Autónoma de Madrid, Campus de Excelencia UAM-CSIC, Cantoblanco, 28049 Madrid, Spain; manuel.yanez@uam.es (M.Y.); otilia.mo@uam.es (O.M.)

* Correspondence: ibon@iqm.csic.es (I.A.); mm.montero@uam.es (M.M.M.-C.)

Academic Editor: Paulo Jorge Costa

Received: 13 November 2019; Accepted: 27 November 2019; Published: 2 December 2019



Abstract: Relativistic effects are found to be important for the estimation of NMR parameters in halogen-bonded complexes, mainly when they involve the heavier elements, iodine and astatine. A detailed study of 60 binary complexes formed between dihalogen molecules (XY with X, Y = F, Cl, Br, I and At) and four Lewis bases (NH₃, H₂O, PH₃ and SH₂) was carried out at the MP2/aug-cc-pVTZ/aug-cc-pVTZ-PP computational level to show the extent of these effects. The NMR parameters (shielding and nuclear quadrupolar coupling constants) were computed using the relativistic Hamiltonian ZORA and compared to the values obtained with a non-relativistic Hamiltonian. The results show a mixture of the importance of the relativistic corrections as both the size of the halogen atom and the proximity of this atom to the basic site of the Lewis base increase.

Keywords: halogen bonding; astatine; relativistic effects; NMR; absolute shieldings; nuclear quadrupolar coupling constants

1. Introduction

Second in importance after hydrogen bonds, halogen bonds (XB) are widely present in many fields such as crystal engineering, biological systems, and the design of new materials, amongst others. It is worth citing here the IUPAC definition of the halogen bond: “A halogen bond occurs when there is evidence of a net attractive interaction between an electrophilic region associated with a halogen atom in a molecular entity and a nucleophilic region in another, or the same, molecular entity” [1]. The properties of this bond have been reviewed in two recent books on this topic [2,3].

A key feature of halogen molecules is the polar flattening of the electron density [4–6], also known as σ -hole [6–8]. This phenomenon is responsible for the directionality of the halogen bond when halogens interact with a Lewis base, a property with an enormous influence on the strength of non-covalent bonds. When combined with other bonds, the same or different, positive and negative cooperativity effects are observed [9–12].

In the gas phase, the experimental evidence of halogen bonds and their properties is usually obtained by microwave spectroscopy. A suitable example is the values reported by Legon et al. by comparing halogen bonds with HBs [13]. In the solid state, this information is obtained by means of nuclear quadrupole resonance techniques, as in the study carried out by Bryce et al. [14–16]. Moreover, relationships between the dissociation energies, D_e , and the nucleophilicity and electrophilicity in XB have been reported [17,18]. Halogen bonds with typical Lewis bases such as phosphines, H₂XP:Cl₂, show traditional and shared halogen bonds [19–21], with the strength of these two kinds of complexes depending on the donor ability of the phosphine.

It is well known that relativistic effects become more and more important when the size of the system increases.

Complexes between halogens and small Lewis donors were usually the simplest models for the study of the halogen bonds, but little work has been done on the relativistic effects on this kind of bond. This can be justified by taking into account that relativistic effects become particularly important when the size of the atoms involved increases. However, in a very interesting paper on chemical shieldings and spin–spin coupling constants, P. Pyykkö clearly showed that relativistic effects were “more common than you thought” [22]; but, for sure, they should be non-negligible when dealing with iodine or astatine derivatives. Even though it was not so common to introduce such effects in the theoretical treatment, [23,24], a recent paper on halogen bonds involving astatine clearly shows the important role these effects may have in the description of the bonds we are dealing with [25].

In this article, the complexes between all the dihalogen molecules including F, Cl, Br, I, and At and four Lewis bases (NH₃, PH₃, H₂O, and SH₂) have been studied (Figure 1). Their dissociation energies, geometries, and NMR properties (chemical shielding and nuclear quadrupole coupling constants) have been obtained and analyzed. Calculations were done using a non-relativistic and a relativistic ZORA Hamiltonian to assess the importance of relativistic effects.

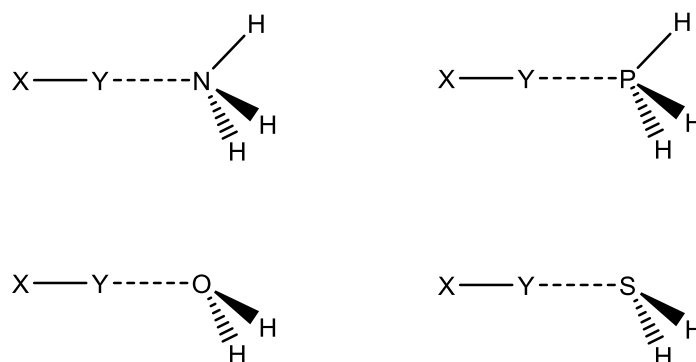


Figure 1. Schematic representation of the complexes studied. (X, Y = F, Cl, Br, I, and At).

2. Computational Methods

The geometry of the complexes was optimized at the MP2 computational level [26] with the aug-cc-pVTZ basis set [27,28]. For iodine and astatine, the effective core potential basis set (ECP) and the aug-cc-pVTZ-PP basis set were used [29]. For complexes involving NH₃ and PH₃, the geometry optimization was done assuming a C_{3v} symmetry and a C_s symmetry for those involving H₂O and SH₂. Vibrational frequency calculations at the same computational level were carried out to confirm that the obtained structures correspond to local minima of the potential energy surface. These calculations were performed with the Gaussian-16 program [30].

In order to provide some insight on the characteristics of the halogen bonds investigated, we decided to use the energy decomposition analysis (EDA) [31] of the interaction energy (Equation (1)), which was carried out with the ADF-2017 program [32] to obtain information of the different energy contributions:

$$E_{\text{int}} = E_{\text{Pauli}} + V_{\text{elst}} + E_{\text{orb}} \quad (1)$$

The Pauli repulsion is associated with the destabilizing interactions between occupied orbitals and is responsible for any steric repulsion. The V_{elst} term corresponds to the classical electrostatic interaction between the two molecules in the geometry of the complexes. The orbital energy, E_{orb} , accounts for the charge transfer and polarization.

Relativistic corrected NMR chemical shieldings and nuclear quadrupole coupling constants (NQCC) were obtained using the full electron QZ4P basis [33], together with the PB86 functional [34–36], and the relativistic ZORA spin-orbit Hamiltonian [37,38]. In addition, non-relativistic calculations

were performed with the same functional and basis set to check the influence of relativistic corrections. For the calculation of the NQCC parameters of astatine, a recently proposed nuclear quadrupole moment of -0.42 barn, was used [39]. These calculations were performed using the ADF-2017 program [32].

The molecular electrostatic potential (MEP) was calculated within the Gaussian-16 facilities and analyzed on the 0.001 au electron density isosurface with the Multiwfn program [40]. The corresponding figures were generated with the JMol program [41]. For the calculation of the MEP no relativistic effects were included, assuming that they will have a small effect on the value of the potential.

3. Results and Discussion

3.1. Isolated Monomers

Prior to the study of the halogen-bonded complexes, an exploration of the properties of the halogen molecules was carried out. The calculated and experimental interatomic distances of the isolated XY molecules are gathered in Table 1. Experimental geometries are available for all the diatomic molecules save for the At derivatives. The calculated values are in good agreement with the experimental ones, the largest error being 0.01 \AA . The calculated and experimental distances show an almost perfect linear correlation ($R^2 = 0.9997$, $n = 10$).

The MEP of these molecules, in agreement with the expected polar flattening already explained in the introduction, presents two σ -holes along the X-Y bond associated with the two atoms (Table 1). In Figure 2, we illustrate the MEP for the particular cases of ClBr and I₂ as representative examples, for which the halo of the lone pairs is easily visualized in red color whereas the σ -hole is markedly blue.

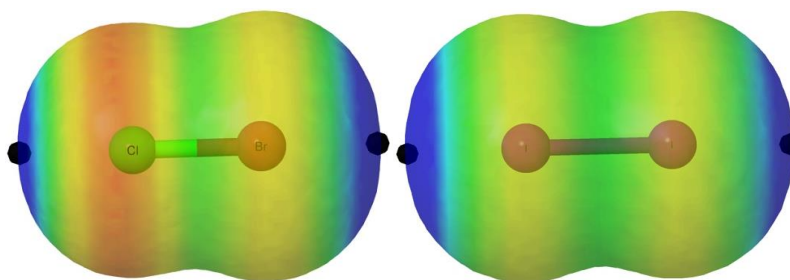


Figure 2. Molecular electrostatic potential (MEP) on the 0.001 a.u. electron density isosurface of the ClBr and I₂ molecules. The location of the σ -hole is indicated with a black dot. The color code range between values > 0.015 au in blue and < -0.010 au in red.

These holes are maxima of the MEP and exhibit positive values. It is important to emphasize, however, that, as already reported in the literature [42], σ -holes do not always present positive MEP values. Indeed, within the systems studied in this work, some of the F derivatives show local maxima with negative values of the MEP. In all cases, the largest σ -hole is associated with the heavier of the two atoms (Y from now on) because of its larger polarizability. For a given Y atom, the value of the σ -hole decreases as the size of X increases, which is associated with a smaller electron withdrawing ability of X. In a series of compounds with the same Y, the changes in the values of the σ -holes follow the changes in the atomic radius of the X atom. Indeed, for Y = At, the largest gap in the value of the σ -hole (0.04 a.u.) is observed on going from F to Cl, with an increase in the atomic radius of 50 pm [43]. Going from Cl to Br, the decrease found in the σ -hole was reduced to 0.012 a.u., with an increase in the atomic radius of only 12 pm . Going from Br to I, the gap between their atomic radii slightly increased (25 pm) and, concomitantly, the gap in the values of the σ -hole (0.017 a.u.) also increased. This finding confirms that the size effects along the periodic table are particularly important when going from the first to the second period. For a given X, the σ -hole increased as the size of the Y atom did, following the increase of the polarizability of the latter. For instance, in the series F₂, FCl, FBr, FI, FAt, the values of the σ -hole increased from 0.0211 a.u. to 0.1310 a.u. (see Table 1).

Table 1. Interatomic distances (Å) and σ -hole values (au) in the isolated X-Y dihalogen molecules.

X-Y	X-Y Distance		σ -Hole	
	Calculated	Experimental [44]	X	Y
F ₂	1.401	1.4119	0.0211	0.0211
FCl	1.638	1.6283	−0.0125 *	0.0762
Cl ₂	1.999	1.9879	0.0434	0.0434
FBr	1.758	1.7589	0.0162	0.0790
ClBr	2.138	2.1360	0.0320	0.0597
Br ₂	2.279	2.2811	0.0485	0.0485
FI	1.920	1.9098	−0.0354 *	0.1103
CII	2.321	2.3209	0.0162	0.0790
BrI	2.465	2.4690	0.0320	0.0686
I ₂	2.663	2.6655	0.0521	0.0521
FAt	2.006		−0.0454 *	0.1310
ClAt	2.407		0.0063	0.0980
BrAt	2.550		0.0217	0.0867
IAt	2.749		0.0419	0.0692
At ₂	2.834		0.0582	0.0582

* These values correspond to local maxima along the F-Y bond.

The nuclear quadrupole coupling constants (NQCC) of the isolated dihalogen molecules are gathered in Table 2. The calculated parameters are in good agreement with the experimental ones.

Table 2. Experimental and calculated values of the nuclear quadrupole coupling constants (NQCC) (MHz) with and without the relativistic ZORA Hamiltonian of the isolated X-Y dihalogen molecules. NR stands for non-relativistic.

X-Y	X Atom				Y Atom			
	Nuclei	Exp. [45]	ZORA	NR	Nuclei	Exp. [45]	ZORA	NR
F ₂	¹⁹ F	a			¹⁹ F			
FCl	¹⁹ F				³⁵ Cl	−145.87182	−146.45	−145.46
Cl ₂	³⁵ Cl	−115.0	−113.27	−112.42	³⁵ Cl	−115.0	−113.27	−112.42
FBr	¹⁹ F				⁷⁹ Br	+1086.89197	1115.10	1060.86
ClBr	³⁵ Cl	−102.378	−103.50	−103.05	⁷⁹ Br	+875.078	903.353	857.40
Br ₂	⁷⁹ Br	+810.0	836.21	792.81	⁷⁹ Br	+810.0	836.21	792.80
FI	¹⁹ F				¹²⁷ I	−3440.748	−3489.90	−3118.75
CII	³⁵ Cl	−85.8	−87.2248	−88.17	¹²⁷ I	−2929.0	−2975.69	−2638.75
BrI	⁷⁹ Br	+722.0	722.50	690.58	¹²⁷ I	−2731.0	−2801.56	−2466.99
I ₂	¹²⁷ I	−2452.5837	−2509.26	−2195.70	¹²⁷ I	−2452.5837	−2509.23	−2195.66
FAt	¹⁹ F				²¹⁰ At		−3553.36	−2788.80
ClAt	³⁵ Cl		−71.0026	−80.93	²¹⁰ At		−3105.21	−212.80
BrAt	⁷⁹ Br		600.699	639.03	²¹⁰ At		−3035.26	−2257.50
IAt	¹²⁷ I		−2172.51	−2049.92	²¹⁰ At		−2738.91	−2025.54
At ₂	²¹⁰ At		−2634.25	−1898.71	²¹⁰ At		−2634.25	−1898.71

^a ¹⁹F has a nullvalue of the nuclear quadrupole moment and consequently the NQCC is always 0.0 MHz.

It should be noted, however, that the deviations of the NR calculated values with respect to the experimental ones are larger than those obtained when relativistic effects are accounted for (ZORA).

As expected, the heavier the halogen atom, the larger the effect. This is seen more clearly when looking at the correlations shown in Figure 3. Indeed, ZORA results present a slightly better R^2 value, a slope closer to 1.0, and an intercept value closer to 0.0 (Figure 3). Negative NQCC values were obtained for the ^{35}Cl , ^{127}I and ^{210}At nucleus, while positive ones were obtained for the ^{79}Br nucleus (as observed in experiments). The positive and negative values of NQCC are associated with the effective shape (prolate and oblate, respectively) of the equivalent ellipsoid of the nuclear charge distribution [46,47]. The absolute average values for each nucleus increased steadily with its size. For a given X (or Y), the NQCC values decreased in absolute value as the size of Y (or X) does.

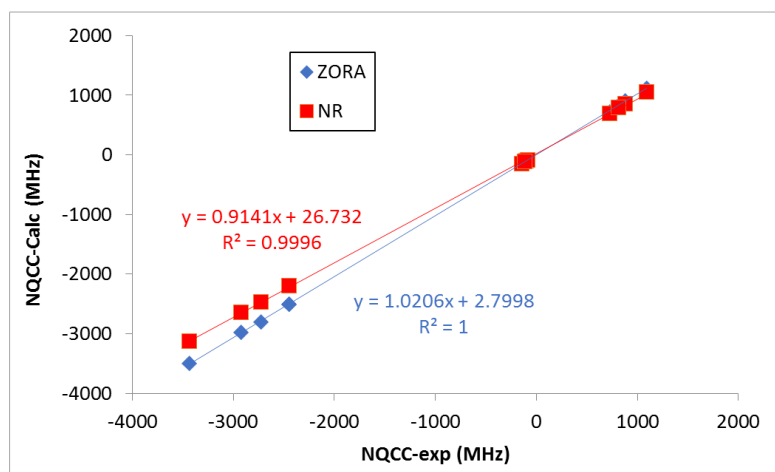


Figure 3. Experimental vs. calculated NQCC parameters (MHz). The fitted linear relationships between the experimental and calculated values are shown.

3.2. Dissociation Energies

Once the properties of the XY molecules were analyzed, we proceeded to study their complexes. The dissociation energies (D_e) of the XY: Base binary complexes are reported in Table 3. The values ranged between $5.6 \text{ kJ}\cdot\text{mol}^{-1}$ for the $\text{F}_2:\text{PH}_3$ and $\text{F}_2:\text{SH}_2$ complexes and $97.7 \text{ kJ}\cdot\text{mol}^{-1}$ for the $\text{FAT}:\text{NH}_3$ complex. Among the trends observed in Table 3, it is interesting to notice that for a given Y atom and base, D_e was smaller as the size of X increased. The largest difference between two consecutive Xs is between F and Cl. Concerning the base, the general trend is $\text{NH}_3 > \text{PH}_3 > \text{SH}_2 > \text{H}_2\text{O}$ with only two exceptions: The $\text{F}_2:\text{OH}_2$ complex that is slightly more stable than the corresponding PH_3 and SH_2 ones, and $\text{FCl}:\text{PH}_3$ that is also slightly more stable than $\text{FCl}:\text{NH}_3$.

The dissociation energies listed in Table 3 can be fitted using Equation (2) proposed by Legon and Millen that relates these energies with a nucleophilic parameter characterizing the bases, N_b , and an electrophilic parameter characterizing the Lewis acids, E_a [17,48,49].

$$D_e = c \cdot N_b \cdot E_a \quad (2)$$

where the constant c has a value of $1.00 \text{ kJ}\cdot\text{mol}^{-1}$ to preserve the units of the equation.

In the present case, we have four N_b values and 15 E_a values to be fitted, so a total of 60 possible combinations. The simultaneous fitting of the nucleophilicities and electrophilicities is done by means of Equation (3).

$$D_e = c \cdot \left(\sum_{i=1}^4 x_i \cdot N_{bi} \right) \cdot \left(\sum_{j=1}^{15} x_j \cdot E_{aj} \right) \quad (3)$$

where the values of x_i and x_j are 1.0 when the corresponding Lewis base or Lewis acid is present in the complex, and 0.0 if it is absent.

The fitted values for each base and acid are given in Table 4. The fitted equation presents a R^2 value of 0.988 and an average unsigned error of $1.7 \text{ kJ}\cdot\text{mol}^{-1}$, the largest error ($7.8 \text{ kJ}\cdot\text{mol}^{-1}$) being found for the $\text{FCl}:\text{PH}_3$ complex. It is known that this complex has a significant ion-pair character $\text{F}^- \cdots \text{ClPH}_3^+$ and, as a consequence, an enhanced D_e [50], which explains this large deviation. Removing the two worst-fitted values ($\text{FCl}:\text{PH}_3$ and $\text{FBr}:\text{PH}_3$), the correlation parameter improved significantly up to $R^2 = 0.994$ with an average error of $1.3 \text{ kJ}\cdot\text{mol}^{-1}$.

Table 3. Dissociation energies (D_e , $\text{kJ}\cdot\text{mol}^{-1}$) of the $\text{XY}:\text{Base}$ complexes.

XY	Base = NH_3	PH_3	H_2O	SH_2
F_2	8.5	5.6	6.0	5.6
FCl	49.5	50.9	23.4	25.8
Cl_2	22.9	14.4	13.2	13.6
FBr	70.2	65.9	35.0	40.1
ClBr	42.2	31.5	22.2	24.0
Br_2	36.0	26.0	19.4	21.3
FI	82.8	71.8	44.4	48.9
ClI	59.8	46.2	31.7	34.3
BrI	53.3	40.1	28.5	30.9
I_2	42.4	30.4	23.2	25.1
FAt	97.7	87.4	55.8	61.6
ClAt	78.7	66.6	43.8	48.4
BrAt	72.2	60.0	40.0	44.4
IAt	61.3	49.2	34.2	37.9
At_2	57.1	46.0	32.0	35.8

The N_b and E_a values obtained for the set of compounds studied here are compared, in Table 4, with others reported in the literature. N_b values in [17] are averaged among 250 complexes including hydrogen bonds, tetrel bonds, pnictogen bonds, chalcogen bonds, and halogen bonds. It is interesting to notice that PH_3 and SH_2 are stronger nucleophiles in halogen bonds than in the rest of the interactions studied in [17]. The same happened in the hydrogen bonds used to fit Equation (2) in [48]. In order to verify whether this increase in the N_b values is due to the presence of the iodine and astatine derivatives not included in [17], we did a new fitting excluding the derivatives of these two elements. The new results of N_b for PH_3 and SH_2 were indeed smaller (6.45 and 4.08, respectively), but the decrease is not significant and the same effect was also observed for the other bases, NH_3 and H_2O (new values 7.25 and 3.67, respectively) not affected by a significant change with respect to the values in [17]. With respect to the E_a values for the dihalogen molecules, they are similar to those reported in [17] since both cases correspond to halogen bonds, though calculated at a slightly different computational level.

The electrostatic nature of these halogen-bonded complexes can be confirmed by comparing the D_e values of all the complexes of a given base with the corresponding σ -hole values associated with the Y atom in the isolated dihalogen molecule (Table 1). Linear correlations between the D_e and σ -hole values, with R^2 between 0.89 and 0.92, were obtained for the complexes with each base. These results clearly improved if the complexes were separated in groups attending to the nature of the Y atom and the base involved in the interaction. Thus, in Figure 4, the relationships for the complexes with iodine and astatine are depicted, showing a linear behavior with $R^2 > 0.99$. These results strongly indicate that other component in addition to electrostatics should be taken into account for a fine-tuning of the estimation of the D_e .

Table 4. Fitted N_b (nucleophilicity) and E_a (electrophilicity) values using the values gathered in Table 3 and Equation (3). The values described in the literature for some of these molecules are also included.

	N_b Value	Ref. [17]	Ref. [48]
NH ₃	8.65	7.52	11.5
PH ₃	7.32	3.12	4.4
H ₂ O	4.70	4.89	10.0
SH ₂	5.19	3.43	4.8
E_a Value			
F ₂	0.97	1.13	
FCl	5.89	5.18	
Cl ₂	2.46	2.71	
FBr	8.24	-	
ClBr	4.65	4.77	
Br ₂	3.96	4.40	
FI	9.61	-	
ClI	6.66	-	
BrI	5.91	-	
I ₂	4.67	-	
FAt	11.65	-	
ClAt	9.16	-	
BrAt	8.35	-	
IAt	7.03	-	
At ₂	6.58	-	

A more detailed analysis of interaction energy was carried out by means of the energy decomposition analysis (Table S1 of the Supporting Information). The results show that the two attractive terms (Pauli and orbital) are important in the stabilization of the complexes, being percentage contributions between 34% and 67% depending on the base and nature of the Y atom, with minimal influence of the X one. The exception to this trend is the FCl:PH₃ complex, where the electrostatic contribution was only 22% and the orbital one 78%. In all the cases, for a given Y atom, the absolute value of the attractive contributions (Pauli, electrostatic and orbitals) decreased as the size of the X atom increased. This is due to the two facts; on the one hand, when X increased, the polarization of Y was smaller, and then the sigma-hole on Y was less deep; and on the other hand, the intermolecular distance increased. For a given X atom, the absolute value of the Pauli and electrostatic contributions increased as the size of Y increases. The FY:PH₃ complexes are an exception to this rule.

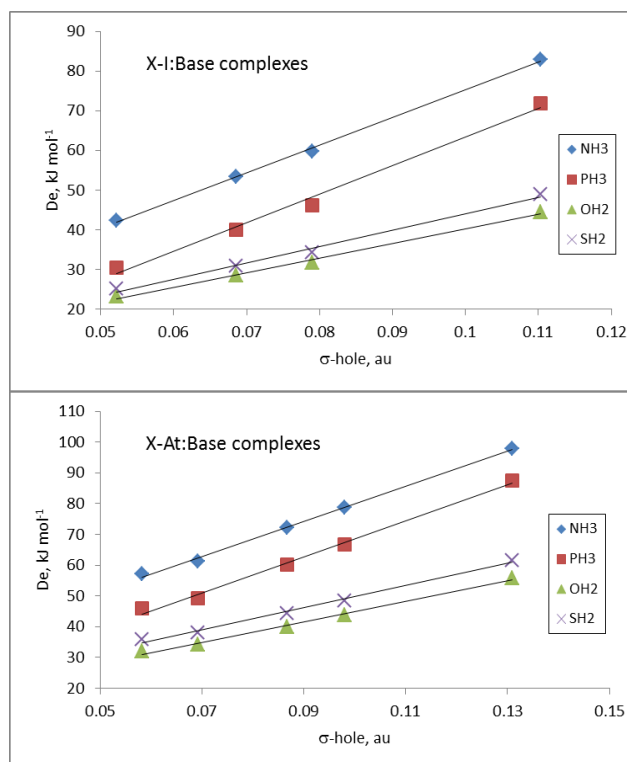


Figure 4. D_e vs. σ -hole in the X-I: Base (**up**) and X-At: Base (**down**) complexes as a function of the Base.

3.3. Halogen Bond Distances

Table 5 collects the halogen bond distances for the whole set of 60 complexes, comparing the MP2/aug-cc-pVTZ values with the experimental ones available in the literature [13,46–48]. The halogen bond distance for the 16 halogen-bonded complexes experimentally known were reasonably well reproduced by our calculations ($R^2 = 0.98$), especially considering that the experimental values included the ZPE effect on the geometry that is not included in the calculations of the optimized geometries. Thus, the calculated values were always shorter than experimental ones in average (0.14 Å).

The calculated halogen bond distances show that in all cases, for a given Y atom and the same base, the distance increased along with the X size because, as mentioned above, the σ -hole at the Y atom became shallower. In general, the distances for the same XY molecule followed the trend $\text{NH}_3 < \text{H}_2\text{O} < \text{PH}_3 < \text{SH}_2$, except in three cases: The F_2 : PH_3 complex showed a slightly larger distance than the F_2 : SH_2 , and the FBr : PH_3 and ClBr : PH_3 distances were shorter than the corresponding one with H_2O . Interestingly, as shown in Table 6, linear correlations $R^2 > 0.92$ were found between the dissociation energies and the halogen bond distances for the complexes with same Y atom and base. The cases of XF and XCl are not included because the number of points is not sufficient.

Table 5. Halogen bond distances (Å) for the XY: Base complexes.

XY	Calculated				Experimental			
	NH ₃	PH ₃	H ₂ O	SH ₂	NH ₃	PH ₃	H ₂ O	SH ₂
F ₂	2.594	3.048	2.649	3.021	2.708 [21]		2.719 [21]	3.200 [13]
FCl	2.233	2.659	2.517	2.721	2.370 [21]		2.611 [13]	2.857 [13]
Cl ₂	2.592	3.050	2.774	3.100	2.730 [21]	3.240 [13]		3.249 [13]
FBr	2.293	2.389	2.493	2.720				
ClBr	2.469	2.659	2.698	2.972	2.628 [13]			3.096 [13]
Br ₂	2.538	2.836	2.757	3.045	2.720 [21]			
FI	2.443	2.642	2.585	2.876				
ClI	2.540	2.792	2.730	3.032	2.711 [51]	2.963 [51]	2.828 [52]	3.154 [51]
BrI	2.582	2.868	2.781	3.087				
I ₂	2.672	3.033	2.869	3.190				
FAt	2.496	2.721	2.593	2.903				
ClAt	2.554	2.802	2.689	3.003				
BrAt	2.582	2.845	2.729	3.041				
IAt	2.640	2.939	2.799	3.116				
At ₂	2.667	2.981	2.828	3.146				

Table 6. R² values for the linear correlations between De and the halogen bond distance.

Base	X-Br:Base	X-I:Base	X-At:Base
NH ₃	0.989	0.967	0.975
PH ₃	0.926	0.918	0.946
H ₂ O	0.998	0.989	0.987
SH ₂	0.994	0.979	0.984

3.4. NMR Absolute Shieldings

The chemical shieldings of the atom of the Lewis base directly involved in the halogen bond are reported in Tables 7 and 8. They were smaller than those in the isolated bases, save in five cases where the relativistic correction was able to revert the trend, as is the case for complexes with FI and FAt.

Table 7. Absolute chemical shielding (ppm) of the atom of the base involved in the interaction. The difference (Δ) between the non-relativistic (NR) and relativistic (ZORA) results is also listed.

XY	NH ₃ Complexes (¹⁵ N NMR)			PH ₃ Complexes (³¹ P NMR)		
	NR	ZORA	Δ	NR	ZORA	Δ
-	259.67	260.59	0.92	569.22	580.5	11.28
F ₂	238.03	239.46	1.43	538.58	550.72	12.14
FCl	222.7	226.35	3.65	444.03	463.76	19.73
Cl ₂	230.4	232.41	2.01	531.28	544.73	13.45
FBr	229.76	245.21	15.45	454.34	500.82	46.48
ClBr	225.08	232.7	7.62	493.61	523.33	29.72
Br ₂	225.15	233.9	8.75	510.84	544.79	33.95
FI	237.04	272.69	35.65	465.54	558.92	93.38
ClI	227.13	246.29	19.16	494.14	549.38	55.24
BrI	224.83	241.62	16.79	504.27	555.62	51.35
I ₂	222.67	238.15	15.48	520.59	568.36	47.77
FAt	241.56	293.55	51.99	472.31	619.06	146.75
ClAt	230.24	258.86	28.62	496.22	573.18	76.96
BrAt	227.03	253.38	26.35	504.9	573.96	69.06
IAt	222.32	249.37	27.05	518.22	585.65	67.43
At ₂	220.25	237.28	17.03	525.75	586.92	61.17

Table 8. ¹⁶O and ³²S absolute shieldings.

XY	H ₂ O Complexes (¹⁶ O NMR)			SH ₂ Complexes (³² S NMR)		
	NR	ZORA	Δ	NR	ZORA	Δ
-	326.51	328.15	1.64	708.5	723.73	15.23
F ₂	311.27	312.88	1.61	660.08	674.88	14.80
FCl	302.28	304.79	2.51	633.48	649.49	16.01
Cl ₂	304.16	306.01	1.85	659.70	674.74	15.04
FBr	308.26	316.74	8.48	636.66	659.18	22.52
ClBr	300.21	303.96	3.75	646.51	664.01	17.50
Br ₂	299.46	303.58	4.12	647.36	663.65	16.29
FI	317.13	337.31	20.18	649.47	682.55	33.08
ClI	300.14	308.94	8.8	645.90	669.24	23.34
BrI	297.5	305.53	8.03	644.13	665.72	21.59
I ₂	294.91	302.81	7.9	642.76	661.24	18.48
FAt	322.85	341	18.15	654.03	693.74	39.71
ClAt	302.38	311.67	9.29	645.26	678.32	33.06
BrAt	297.8	308.72	10.92	641.84	676.2	34.36
IAt	291.66	307.79	16.13	636.52	673.34	36.82
At ₂	288.79	298.26	9.47	633.27	655.14	21.87

The relativistic correction was always positive with values up to 147 ppm in the FAt:PH₃ complex. Although no clear correlations were found between the intermolecular distances and the non-relativistic

chemical shieldings, a clear dependence with the distance and the nuclei was observed for the values including relativistic corrections (see Figure 5).

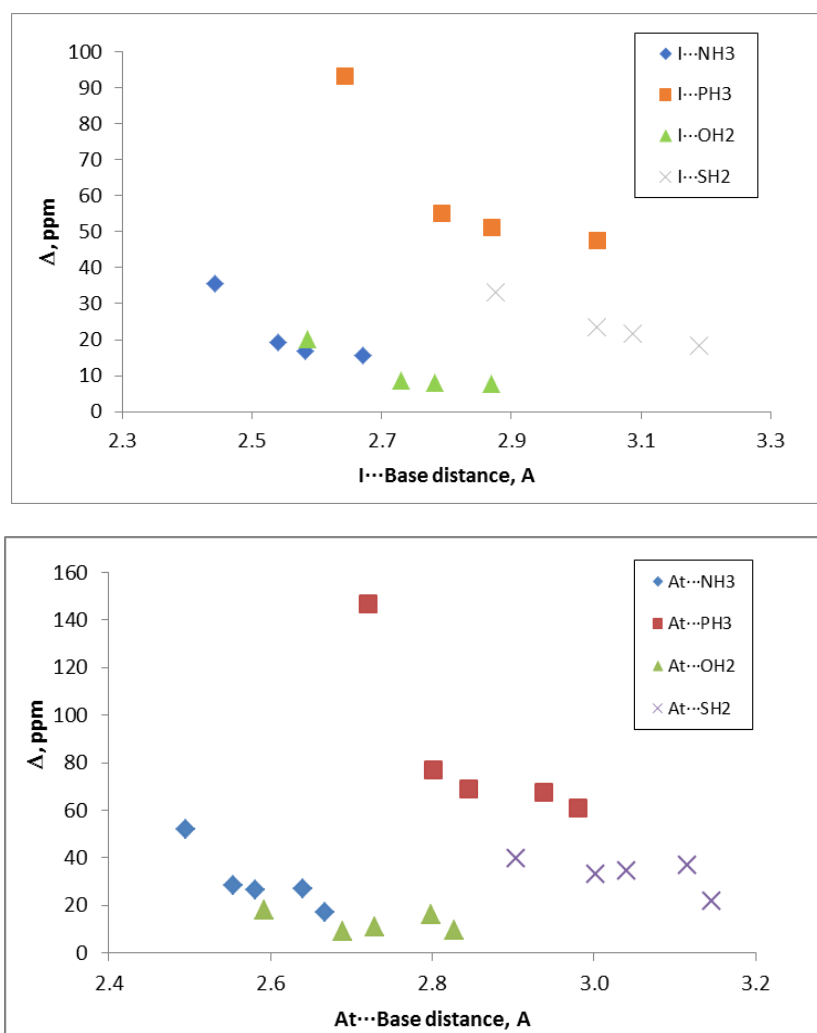


Figure 5. Relativistic effect on the chemical shielding, Δ , of the base on I: Base and At: Base interactions vs. the intermolecular distance.

3.5. NQCC

The NQCC values of the halogen atoms XY in the binary complexes calculated with the ZORA Hamiltonian are gathered in Table 9. Remember that ^{19}F has no NQCC. Significant variations of this parameter were observed for both nuclei X and Y upon complexation. In the case of X, positive variations with respect to the corresponding value in the isolated XY molecules (see Table 2) were observed for the ^{35}Cl , ^{127}I , and ^{210}At nuclei while negative variations were found for the ^{79}Br one. Thus, the absolute values of the binary complexes were, from 7 to 831 MHz, smaller than the ones in the isolated XY molecules. For a given Y and base, the variation in absolute value followed the sequence $\text{Cl} < \text{Br} < \text{I} < \text{At}$. For a given XY molecule, the variation of the NQCC of X, with respect to the base, was larger in NH_3 and PH_3 than SH_2 , the complexes with H_2O being the ones with the smallest variations.

Table 9. NQCC values (MHz) for the X (a) and Y (b) atoms in the XY: Base binary complexes.

XY	X Nuclei	Base = NH ₃	PH ₃	H ₂ O	SH ₂
F ₂	¹⁹ F	-	-	-	-
FCl	¹⁹ F	-	-	-	-
Cl ₂	³⁵ Cl	-96.67	-101.60	-106.45	-103.33
FBr	¹⁹ F	-	-	-	-
ClBr	³⁵ Cl	-80.73	-75.90	-94.06	-89.17
Br ₂	⁷⁹ Br	666.62	669.73	766.09	731.14
FI	¹⁹ F	-	-	-	-
ClI	³⁵ Cl	-65.83	-62.74	-77.20	-73.07
BrI	⁷⁹ Br	550.33	539.92	643.91	611.72
I ₂	¹²⁷ I	-1978.37	-2027.60	-2275.95	-2182.00
FAt	¹⁹ F	-	-	-	-
ClAt	³⁵ Cl	-53.71	-51.30	-61.91	-58.97
BrAt	⁷⁹ Br	453.45	439.72	524.63	500.39
IAt	¹²⁷ I	-1656.06	-1651.19	-1912.51	-1833.11
At ₂	²¹⁰ At	-2020.99	-2009.78	-2220.53	-1803.44

(a)

XY	Y-Nuclei	Base = NH ₃	PH ₃	H ₂ O	SH ₂
F ₂	¹⁹ F	-	-	-	-
FCl	³⁵ Cl	-136.74	-104.16	-144.73	-136.22
Cl ₂	³⁵ Cl	-113.90	-111.54	-114.86	-111.80
FBr	⁷⁹ Br	1031.94	861.95	1093.30	1017.95
ClBr	⁷⁹ Br	898.39	832.30	914.18	877.07
Br ₂	⁷⁹ Br	841.11	799.32	850.08	818.11
FI	¹²⁷ I	-3292.39	-2920.15	-3453.39	-3239.75
ClI	¹²⁷ I	-2968.23	-2745.65	-3024.02	-2888.87
BrI	¹²⁷ I	-2823.84	-2641.50	-2859.06	-2738.31
I ₂	¹²⁷ I	-2583.75	-2457.53	-2582.64	-2490.00
FAt	²¹⁰ At	-3603.13	-3254.61	-3613.52	-3400.17
ClAt	²¹⁰ At	-3275.35	-3054.35	-3209.75	-3108.67
BrAt	²¹⁰ At	-3056.78	-2950.25	-3129.21	-3071.55
IAt	²¹⁰ At	-2977.79	-2799.42	-2883.22	-2768.93
At ₂	²¹⁰ At	-2921.46	-2688.23	-2748.77	-2588.70

(b)

In the case of Y, the variation was more negative (or less positive) as the size of the X atom increased for ³⁵Cl and ¹²⁷I, while for ⁷⁹Br and ²¹⁰At nuclei, the reverse trend was observed.

Recently, a relationship has been explored between the variation of the NQCC of the dihalogen molecules isolated and in complexes and the charge redistribution using the Townes–Dailey model [53]. Similar results have been obtained from the theoretical charge distribution obtained within the atoms in molecules methodology [54].

4. Conclusions

NMR and NQCC parameters, dissociation energies, and intermolecular distances were studied in detail for 60 halogen-bonded complexes between XY halogen molecules and a set of Lewis bases, namely NH₃, PH₃, SH₂, and H₂O, taking into account relativistic effects. Isolated halogen molecules exhibited negative NQCC values for ³⁵Cl, ¹²⁷I, and ²¹⁰At nucleus, and positive ones for ⁷⁹Br; the bigger the atom, the larger the absolute NQCC value. In the binary complexes XY: Base, the NQCCs calculated for X, including relativistic effects, present positive variations with respect to isolated XY molecule for ³⁵Cl, ¹²⁷I, and ²¹⁰At, and negative for ⁷⁹Br. This implies a reduction in absolute value of the NQCCs with respect to isolated halogens for all the nuclei, the variation following the trend Cl < Br < I < At. Among the Lewis bases, for a same XY molecule, NH₃ and H₂O led to the largest and shortest variations, respectively. On the other hand, the chemical shieldings of the atoms of the bases directly involved in the interaction were smaller than in the isolated bases, with some exceptions where the relativistic correction reverts the trend. This relativistic correction is always positive, reaching the highest value (147 ppm) for the FAt:PH₃ complex.

Regarding the energy of the halogen-bonded complexes, molecular fluorine complexes show the smallest dissociation energies (5.6 kJ·mol⁻¹ for both F₂:PH₃ and F₂:SH₂) and the FAt complexes the largest ones (97.7 kJ·mol⁻¹ for FAt: NH₃). Again, the general trend shows that NH₃ leads to the strongest complexes and H₂O to the weakest ones, with few exceptions. Dissociation energies fit well with nucleophilicity and electrophilicity parameters proposed by Legon (R² = 0.994 if only two anomalous values are removed from the fitting). The importance of electrostatics is evidenced by the fact that dissociation energies and σ -hole MEP values of halogens are mostly linearly correlated (R² = 0.89–0.92), but for complexes with iodine and astatine, this correlation is almost perfect (R² > 0.99), indicating that not only electrostatic factors should be taken into account for smaller halogens.

Supplementary Materials: The following are available online at <http://www.mdpi.com/1420-3049/24/23/4399/s1>: Information regarding coordinates and MP2 energies.

Author Contributions: I.A. did the calculations. All authors (I.A., J.E., M.Y., O.M., and M.M.M.-C.) analyzed and discussed the results and commented on the manuscript and contributed equally to the writing of this paper.

Funding: Financial support from the Ministerio de Ciencia, Innovación y Universidades (projects PGC2018-094644-B-C21, PGC2018-094644-B-C22 and CTQ2016-76061-P) and Comunidad de Madrid (P2018/EMT-4329 AIRTEC-CM). The authors want to thank the CTI (CSIC) for the computational resources.

Conflicts of Interest: The authors declare no conflict of interest.

References

1. Desiraju, G.R.; Ho, P.S.; Kloo, L.; Legon, A.C.; Marquardt, R.; Metrangolo, P.; Politzer, P.; Resnati, G.; Rissanen, K. Definition of the halogen bond (IUPAC Recommendations 2013). *Pure Appl. Chem.* **2013**, *85*, 1711–1713. [[CrossRef](#)]
2. Metrangolo, P.; Resnati, G. Halogen bonding. fundamentals and applications. *Struct. Bond.* **2008**, *126*.
3. Metrangolo, P.; Resnati, G. Halogen bonding, I. impact on materials chemistry and life sciences. *Top. Curr. Chem.* **2015**, *358*.
4. Sedlak, R.; Kolár, M.H.; Hobza, P. Polar flattening and the strength of halogen bonding. *J. Chem. Theor. Comput.* **2015**, *11*, 4727–4732. [[CrossRef](#)] [[PubMed](#)]
5. Kolár, M.H.; Hobza, P. Computer modeling of halogen bonds and other σ -hole interactions. *Chem. Rev.* **2016**, *116*, 5155–5187. [[CrossRef](#)] [[PubMed](#)]
6. Clark, T. Halogen bonds and σ -holes. *Faraday Discuss.* **2017**, *203*, 9–27. [[CrossRef](#)] [[PubMed](#)]
7. Politzer, P.; Murray, J.S.; Clark, T. Halogen bonding: An electrostatically-driven highly directional noncovalent interaction. *Phys. Chem. Chem. Phys.* **2010**, *12*, 7748–7757. [[CrossRef](#)]
8. Politzer, P.; Murray, J.S. Halogen bonding and other σ -hole interactions: A perspective. *Phys. Chem. Chem. Phys.* **2013**, *15*, 11178–11189. [[CrossRef](#)]
9. Grabowski, S.J.; Bilewicz, E. Cooperativity Halogen Bonding Effect-Ab initio Calculations on H₂CO⋯(ClF)_n Complexes. *Chem. Phys. Lett.* **2006**, *427*, 51–55. [[CrossRef](#)]

10. Solimannejad, M.; Malekani, M.; Alkorta, I. Substituent effects on the cooperativity of halogen bonding. *J. Phys. Chem. A* **2013**, *117*, 5551–5557. [[CrossRef](#)]
11. Alkorta, I.; Blanco, F.; Deyà, P.M.; Elguero, J.; Estarellas, C.; Frontera, A.; Quiñonero, D. Cooperativity in multiple unusual weak bonds. *Theor. Chem. Acc.* **2010**, *126*, 1–14. [[CrossRef](#)]
12. Bauzá, A.; Frontera, A. On the importance of halogen-halogen interactions in the solid state of fullerene halides: A combined theoretical and crystallographic study. *Crystals* **2016**, *6*, 191. [[CrossRef](#)]
13. Legon, A.C. Prereactive complexes of dihalogens XY with Lewis bases B in the gas phase: A systematic case for the halogen analogue B··XY of the hydrogen bond B··HX. *Angew. Chem. Int. Ed.* **1999**, *38*, 2686–2714. [[CrossRef](#)]
14. Xu, Y.; Huang, J.; Gabidullin, B.; Bryce, D.L. A rare example of a phosphine as a halogen bond acceptor. *Chem. Commun.* **2018**, *54*, 11041–11043. [[CrossRef](#)]
15. Xu, Y.; Gabidullin, B.; Bryce, D.L. Single-Crystal NMR characterization of halogen bonds. *J. Phys. Chem. A* **2019**, *123*, 6194–6209. [[CrossRef](#)]
16. Szell, P.M.J.; Zablony, S.; Bryce, D.L. Halogen bonding as a supramolecular dynamics catalyst. *Nat. Commun.* **2019**, *10*, 916. [[CrossRef](#)]
17. Alkorta, I.; Legon, A.C. Nucleophilicities of Lewis bases B and electrophilicities of Lewis acids a determined from the dissociation energies of complexes B··A involving hydrogen bonds, tetrel bonds, pnictogen bonds, chalcogen bonds and halogen bonds. *Molecules* **2017**, *22*, 1786. [[CrossRef](#)]
18. Shaw, R.A.; Hill, J.G. A simple model for halogen bond interaction energies. *Inorganics* **2019**, *7*, 19. [[CrossRef](#)]
19. Alkorta, I.; Elguero, J.; Del Bene, J. Characterizing traditional and chlorine-shared halogen bonds in complexes of phosphine derivatives with ClF and Cl₂. *J. Phys. Chem. A* **2014**, *118*, 4222–4231. [[CrossRef](#)]
20. Del Bene, J.E.; Alkorta, I.; Elguero, J. Influence of substituent effects on the formation of p··cl pnictogen bonds or halogen bonds. *J. Phys. Chem. A* **2014**, *118*, 2360–2366. [[CrossRef](#)]
21. Shaw, R.A.; Hill, J.G.; Legon, A.C. Halogen bonding with phosphine: Evidence for mulliken inner complexes and the importance of relaxation energy. *J. Phys. Chem. A* **2016**, *120*, 8461–8468. [[CrossRef](#)] [[PubMed](#)]
22. Pyykkö, P. Relativistic effects in chemistry: More common than you thought. *Ann. Rev. Phys. Chem.* **2012**, *63*, 45–64. [[CrossRef](#)] [[PubMed](#)]
23. Dojahn, J.G.; Chen, E.C.M.; Wentworth, W.E. Characterization of homonuclear diatomic ions by semiempirical morse potential energy curves. 1. the halogen anions. *J. Phys. Chem.* **1996**, *100*, 9649–9657. [[CrossRef](#)]
24. Alkorta, I.; Blanco, F.; Solimannejad, M.; Elguero, J. Competition of hydrogen bonds and halogen bonds in complexes of hypohalous acids with nitrogenated bases. *J. Phys. Chem. A* **2008**, *112*, 10856–10863. [[CrossRef](#)]
25. Guo, N.; Maurice, R.; Teze, D.; Graton, J.; Champion, J.; Montavoni, G.; Galland, N. Experimental and computational evidence of halogen bonds involving astatine. *Nat. Chem.* **2018**, *10*, 428–434. [[CrossRef](#)]
26. Møller, C.; Plesset, M.S. Note on an approximation treatment for many-electron systems. *Phys. Rev.* **1934**, *46*, 618–622. [[CrossRef](#)]
27. Woon, D.E.; Dunning, T.H. Gaussian basis sets for use in correlated molecular calculations. V. Core-valence basis sets for boron through neon. *J. Chem. Phys.* **1995**, *103*, 4572–4585. [[CrossRef](#)]
28. Dunning, T.H. Gaussian-Basis sets for use in correlated molecular calculations 1. The atoms boron through neon and hydrogen. *J. Chem. Phys.* **1989**, *90*, 1007–1023. [[CrossRef](#)]
29. Peterson, K.A. Systematically convergent basis sets with relativistic pseudopotentials. II. Small-core pseudopotentials and correlation consistent basis sets for the post-d group 16–18 elements. *J. Chem. Phys.* **2003**, *119*, 11113–11123. [[CrossRef](#)]
30. Frisch, M.J.; Trucks, G.W.; Schlegel, H.B.; Scuseria, G.E.; Robb, M.A.; Cheeseman, J.R.; Scalmani, G.; Barone, V.; Petersson, G.A.; Nakatsuji, H.; et al. *Gaussian 16*; Gaussian, Inc.: Wallingford, CT, USA, 2016.
31. Ziegler, T.; Rauk, A. Theoretical- study of the ethylene-metal bond in complexes between Cu⁺, Ag⁺, Au⁺, Pt⁰, or Pt²⁺ and ethylene, based on the Hartree-Fock-Slater transition-state method. *Inorg. Chem.* **1979**, *18*, 1558–1564. [[CrossRef](#)]
32. Te Velde, G.; Bickelhaupt, F.M.; Baerends, E.J.; Fonseca Guerra, C.S.; van Gisbergen, J.A.; Snijders, J.G.; Ziegler, T. Chemistry with ADF. *J. Comput. Chem.* **2001**, *22*, 931–967. [[CrossRef](#)]
33. Van Lenthe, E.; Baerends, E.J. Optimized Slater-type basis sets for the elements 1–118. *J. Comput. Chem.* **2003**, *24*, 1142–1156. [[CrossRef](#)] [[PubMed](#)]
34. Vosko, S.H.; Wilk, L.; Nusair, M. Accurate spin-dependent electron liquid correlation energies for local spin density calculations: A critical analysis. *Can. J. Phys.* **1980**, *58*, 1200–1211. [[CrossRef](#)]

35. Becke, A. Density-functional exchange-energy approximation with correct asymptotic behavior. *Phys. Rev. A: At. Mol. Opt. Phys.* **1988**, *38*, 3098–3100. [CrossRef] [PubMed]
36. Perdew, J.P. Density-functional approximation for the correlation energy of the inhomogeneous electron gas. *Phys. Rev. B* **1986**, *33*, 8822. [CrossRef]
37. Schreckenbach, G.; Ziegler, T. Calculation of NMR shielding tensors using gauge-including atomic orbitals and modern density functional theory. *J. Phys. Chem.* **1995**, *99*, 606–611. [CrossRef]
38. van Lenthe, E.; Baerends, E.J.; Snijders, J.G. Relativistic regular two-component Hamiltonians. *J. Chem. Phys.* **1993**, *99*, 4597–4610. [CrossRef]
39. Cubiss, J.G.; Barzakh, A.E.; Seliverstov, M.D.; Andreyev, A.N.; Andel, B.; Antalic, S.; Ascher, P.; Atanasov, D.; Beck, D.; Bieroń, J.; et al. Charge radii and electromagnetic moments of ^{195–211}At. *Phys. Rev. C* **2018**, *97*, 054327. [CrossRef]
40. Lu, T.; Chen, F. Multiwfn: A multifunctional wavefunction analyzer. *J. Comput. Chem.* **2012**, *33*, 580–592. [CrossRef]
41. Jmol: An Open-source Java Viewer for Chemical Structures in 3D. Available online: <http://jmol.sourceforge.net> (accessed on 13 November 2019).
42. Rezac, J.; Riley, K.E.; Hobza, P. Benchmark calculations of noncovalent interactions of halogenated molecules. *J. Chem. Theory Comput.* **2012**, *8*, 4285–4292. [CrossRef]
43. Slater, J.C. Atomic radii in crystals. *J. Chem. Phys.* **1964**, *41*, 3199–3205. [CrossRef]
44. NIST Computational Chemistry Comparison and Benchmark Database. NIST Standard Reference Database Number 101. Release 20, August 2019, Editor: Russell, D. Johnson III. Available online: <http://cccbdb.nist.gov> (accessed on 13 November 2019).
45. Palmer, M.H.; Blair-Fish, J.A.; Sherwood, P.; Guest, M.F. Halogen nuclear quadrupole coupling constants: Comparison of ab initio calculations which include correlation, with experiment. *Z. Naturforsch.* **1998**, *53*, 383–395. [CrossRef]
46. Physical chemistry division commission on molecular structure and spectroscopy. Nomenclature and conventions for reporting mossbauer spectroscopic data. *Pure Appl. Chem.* **1976**, *45*, 211–216. [CrossRef]
47. Autschbach, J.; Zheng, S.; Schurko, R.W. Analysis of electric field gradient tensors at quadrupolar nuclei in common structural motifs. *Concepts Magn. Reson. Part A* **2010**, *36*, 84–126. [CrossRef]
48. Legon, A.C.; Millen, D.J. Hydrogen bonding as a probe of electron densities: Limiting gas-phase nucleophilicities and electrophilicities of B and HX. *J. Am. Chem. Soc.* **1987**, *109*, 356–358. [CrossRef]
49. Alkorta, I.; Legon, A.C. Non-Covalent interactions involving alkaline-earth atoms and lewis bases b: An ab initio investigation of beryllium and magnesium bonds, B··MR₂ (M = Be or Mg, and R = H, F or CH₃). *Inorganics* **2019**, *7*, 35. [CrossRef]
50. Alkorta, I.; Rozas, I.; Elguero, J. Charge-Transfer complexes between dihalogen compounds and electron donors. *J. Phys. Chem. A* **1998**, *102*, 9278–9285. [CrossRef]
51. Hill, J.G.; Legon, A.C.; Tew, D.P.; Walker, N.R. Halogen bonding in the gas phase: A comparison of the iodine bond in B··ICl and B··ICF₃ for simple Lewis bases, B. *Top. Curr. Chem.* **2015**, *358*, 43–77.
52. Davey, J.B.; Legon, A.C.; Waclawik, E.R. An investigation of the gas-phase complex of water and iodine monochloride by microwave spectroscopy: Geometry, binding strength and electron redistribution. *Phys. Chem. Chem. Phys.* **2000**, *2*, 1659–1665. [CrossRef]
53. Townes, C.H.; Dailey, B.P. Determination of electronic structure of molecules from nuclear quadrupole effects. *J. Chem. Phys.* **1949**, *17*, 782–796. [CrossRef]
54. Alkorta, I.; Legon, A.C. Systematic behaviour of electron redistribution on formation of halogen-bonded complexes B··XY, as determined via XY halogen nuclear quadrupole coupling constants. *Phys. Chem. Chem. Phys.* **2019**, *21*, 16914–16922. [CrossRef] [PubMed]

